Crenulation-slip development in a Caledonian shear zone in NW Ireland: evidence for a multi-stage movement history

D. M. Chew, J. S. Daly, M. J. Flowerdew, M. J. Kennedy and L. M. Page

Geological Society, London, Special Publications 2004; v. 224; p. 337-352
doi:10.1144/GSL.SP.2004.224.01.21

Crenulation-slip development in a Caledonian shear zone in NW Ireland: evidence for a multi-stage movement history

D. M. CHEW[1], J. S. DALY[2], M. J. FLOWERDEW[3], M. J. KENNEDY[2] & L. M. PAGE[4,5]

[1]*Département de Minéralogie, Université de Genève, Rue des Maraîchers 13, CH-1205 Genève, Switzerland (e-mail: david.chew@terre.unige.ch)*

[2]*Department of Geology, University College Dublin, Belfield, Dublin 4, Ireland*

[3]*British Antarctic Survey, c/o NERC Isotope Geosciences Laboratory, Kingsley Dunham Centre, Keyworth, Nottingham NG12 5GG, UK*

[4]*Laboratory of Isotope Geology, Vrije Universiteit, De Boelelaan 1085, 1081 HV Amsterdam, the Netherlands*

[5]*Present address: Department of Geology, Lund University, Sölvegatan 13, 223 62 Lund, Sweden*

Abstract: In Scotland and Ireland, a Laurentian passive margin sequence, the Dalradian Supergroup, was deformed during the *c.* 470–460 Ma Grampian orogeny, resulting in the formation of crustal-scale recumbent nappes. In Ireland, this passive margin sequence is in general bounded to the SE by the Fair Head–Clew Bay Line (FHCBL), a segment of a major lineament within the Caledonides. Adjacent to the FHCBL, Dalradian metasediments in two separate inliers have undergone post-Grampian strike–slip movement, with the initially flat-lying Grampian nappe fabric acting as a décollement-like slip surface in both cases. As the orientation of these foliation slip surfaces was oblique to the local shear plane in both inliers, displacement along these pre-existing foliation surfaces was also accompanied by crenulation slip. However, the crenulation-slip morphologies produced imply the opposite sense of movement in the two inliers. ^{40}Ar–^{39}Ar dating of muscovite defining the crenulation-slip surfaces indicates that post-Grampian dextral displacement took place along the FHCBL at 448 ± 3 Ma. A subsequent phase of sinistral movement along the FHCBL took place at *c.* 400 Ma, based on previously published Rb–Sr muscovite ages for synkinematic pegmatites. The kinematic information obtained from crenulation-slip morphologies combined with geochronology can thus be used to constrain the reactivation history of a major crustal-scale shear zone.

Deforming materials are seldom isotropic, and hence anisotropy plays an important role in partitioning strain in shear zones. Common examples of anisotropy encountered in mid-crustal shear zones include planar elements such as sedimentary layering or foliations. Such planar anisotropies should act as décollement-like surfaces during shear deformation when they are suitably orientated (i.e. subparallel to the shear plane). Renewed movement along pre-existing foliations (foliation reactivation) is thus likely to be a feature of many mid-crustal shear zones.

Kinematic models have been used (e.g. Dennis & Secor 1987) to predict the structural features produced when slip occurs along foliation surfaces which are oblique to the walls of a shear zone. Oblique slip produces a displacement component normal to the zone wall, which is inconsistent with plane strain, simple shear deformation (Ramsay & Graham 1970). In order to maintain the initial thickness of the shear zone and thus preserve a simple shear deformation path, crenulation slip has been interpreted to compensate for this normal displacement component (Dennis & Secor 1987).

This paper presents structural and ^{40}Ar–^{39}Ar and Rb–Sr isotopic data from a major shear zone within the Caledonides of NW Ireland, the Fair Head–Clew Bay Line. Detailed field mapping has demonstrated that the main regional foliation developed within Dalradian Supergroup metasediments adjacent to the Fair Head–Clew Bay Line is used as a slip surface within this shear zone, where it is accompanied by crenulation slip. The age of the main regional foliation is also well constrained by previous geochronological studies based immediately outside this shear zone (e.g. Flowerdew *et al.* 2000; Chew *et al.* 2003), where it is unaffected by later

From: ALSOP, G. I., HOLDSWORTH, R. E., MCCAFFREY, K. J. W. & HAND, M. (eds) 2004. *Flow Processes in Faults and Shear Zones*. Geological Society, London, Special Publications, **224**, 337–352. 0305-8719/$15.00

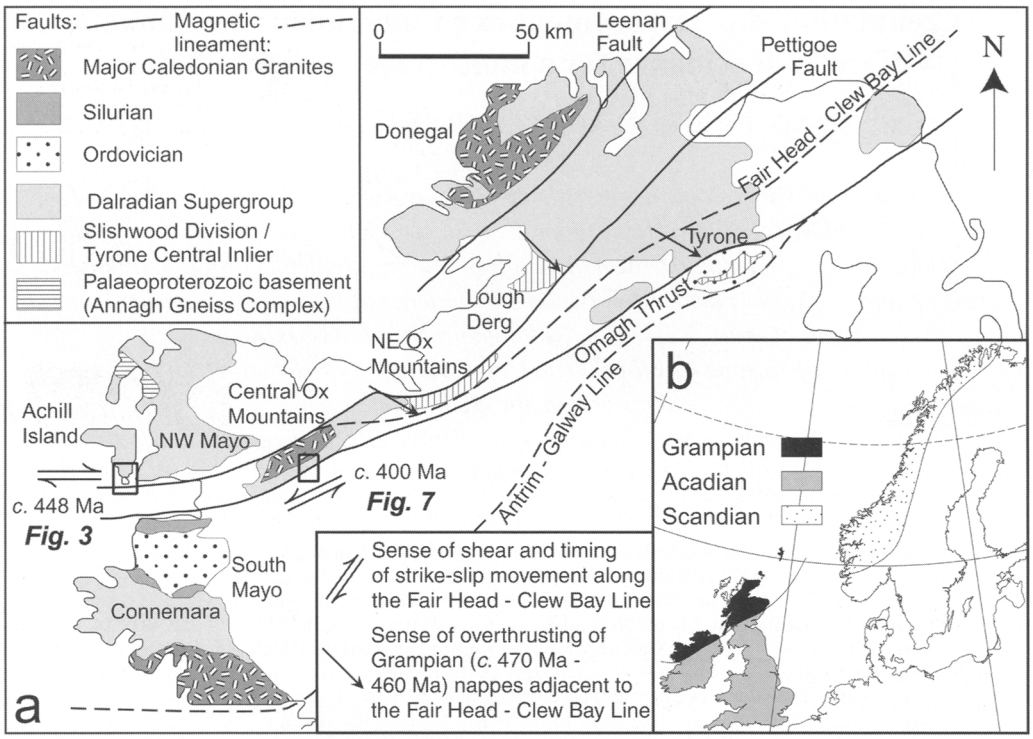

Fig. 1. (**a**) Regional geology of NW Ireland displaying localities referred to in the text. (**b**) Location map of Ireland within the Caledonides.

deformation (i.e. shearing). Isotopic dating of both the crenulation-slip fabrics and the reactivated foliation within the shear zone enable individual phases of reactivation to be constrained temporally. The crenulation morphologies predicted by the model described above can thus be used to identify not only shear sense on a major crustal-scale shear zone, but also to establish the timing of movement.

Geological significance of the Fair Head–Clew Bay Line

In NW Ireland, a Laurentian passive margin sequence, the Neoproterozoic–Cambrian Dalradian Supergroup (Fig. 1), was deformed during the *c.* 470–460 Ma Grampian orogeny (Friedrich *et al.* 1999*a*, *b*; Flowerdew *et al.* 2000). This orogenic episode is believed to be related to the collision of the Laurentian margin with an outboard oceanic arc and associated forearc ophiolite (Dewey & Shackleton 1984), which resulted in metamorphism and the production of crustal-scale recumbent nappes within the Dalradian sequence.

The Dalradian Supergroup in NW Ireland (with the exception of the allochthonous Connemara terrane) is bounded to the SE by the Fair Head–Clew Bay Line (Fig. 1). This structure is believed to be equivalent to the Highland Boundary Fault of Scotland and the Baie Verte–Brompton Line of Newfoundland and as such is a significant lineament within the Caledonides. It is believed to represent the original collisional suture between the deformed and metamorphosed Laurentian margin sequences and the outboard oceanic arc (Dewey & Shackleton 1984).

The Fair Head–Clew Bay Line itself is defined by a conspicuous magnetic lineament (Max & Riddihough 1975) from northeastern Ireland (Fig. 1) to the north shore of Clew Bay on the western Irish coast (Fig. 2a), whereas the main surface expression of the Fair Head–Clew Bay Line is a fault zone which in general lies about 10 km to the south of the magnetic lineament (Fig. 1). Both are often collectively referred to as the Fair Head–Clew Bay Line (Ryan *et al.* 1995).

Throughout most of the southeastern margin of the Dalradian Supergroup in Scotland and Ireland, ductile structures related to movement

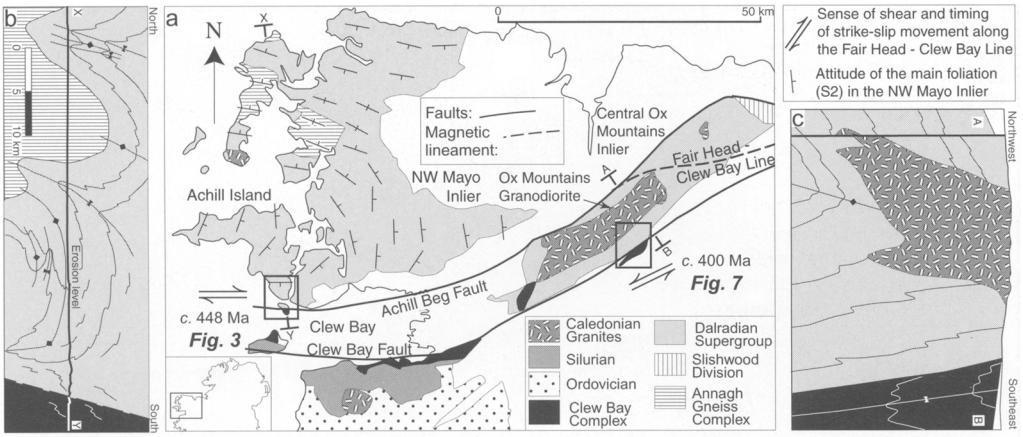

Fig. 2. (**a**) Regional geology of Co. Mayo displaying localities referred to in the text. (**b**) North–south cross-section (X–Y) across the NW Mayo inlier displaying major F_2 folds. (**c**) NW–SE cross section across the Central Ox Mountains inlier adapted from MacDermot *et al.* (1996) and displaying major F_3 folds.

along the Highland Boundary Fault or the Fair Head–Clew Bay Line are rarely exposed. However, in Dalradian Supergroup metasediments on Achill Island in NW Mayo and in the Central Ox Mountains (Fig. 1), ductile structures which can be related to strike–slip motion along the Fair Head–Clew Bay Line (FHCBL) are clearly observed.

Evidence for strike–slip motion along the FHCBL in NW Mayo (South Achill)

Achill Island is situated on the southern margin of the NW Mayo inlier (Figs 1 & 2a). The NW Mayo inlier preserves an excellently exposed transect from Laurentian basement, the Annagh Gneiss Complex (Daly 1996), through presumed para-autochthonous (Winchester 1992) Laurentian cover, the Dalradian Supergroup, to outboard oceanic elements located immediately to the south of the FHCBL (e.g. the Clew Bay Complex; Williams *et al.* 1994).

Polyphase deformation is pervasive throughout the Dalradian Supergroup outcrop in Ireland and Scotland. In the NW Mayo inlier, a D_1 deformation event is responsible for the bulk of the high-strain observed, and is associated with the development of tectonic slides and locally-developed isoclinal F_1 folds (Kennedy 1980). The D_2 deformation event in the NW Mayo inlier is the main nappe-forming phase. The D_2 nappes in general plunge gently east and 'root' in the basement core, the Annagh Gneiss Complex (Fig. 2b). Adjacent to, and directly above the Annagh Gneiss Complex, the D_2 nappes are upward-facing (Fig. 2b); to the south of this 'root zone' recumbent D_2 folds face south (Fig. 2b; Kennedy 1980) and are rotated into a downward-facing orientation approaching the southern margin of the inlier (Fig. 2b; Chew 2003). The production of downward-facing D_2 folds and the associated S_2 strike-swing (Fig. 2a) in the southern part of the inlier has been attributed to either later modification of the D_2 nappe pile by an east–west dextral shear zone running along the north margin of Clew Bay (Sanderson *et al.* 1980; Chew 2003), or a steep zone of D_2 dextral transpression contemporaneous with the development of flat-lying D_2 nappes to the north (Harris 1993, 1995).

The model of Sanderson *et al.* (1980) assumed that the S_2 nappe fabric was progressively rotated into the proposed shear zone rather than new fabrics forming. However, detailed mapping of the southern part of Achill Island (South Achill) and the island of Achill Beg (Fig. 3) on the southern margin of the inlier demonstrates that the S_2 nappe fabric is modified by D_3 structures consistent with dextral strike–slip displacement. The northern boundary of the shear zone to the north is not sharply defined, but D_3 structures gradually become less abundant to the north of Ashleam Bay in South Achill (Fig. 3). Two discrete elements have been recognized in the D_3 deformation episode, asymmetrical buckle folds with axial planes anticlockwise to the S_2 foliation, and extensional crenulation cleavages which cut the S_2 foliation in a clockwise sense.

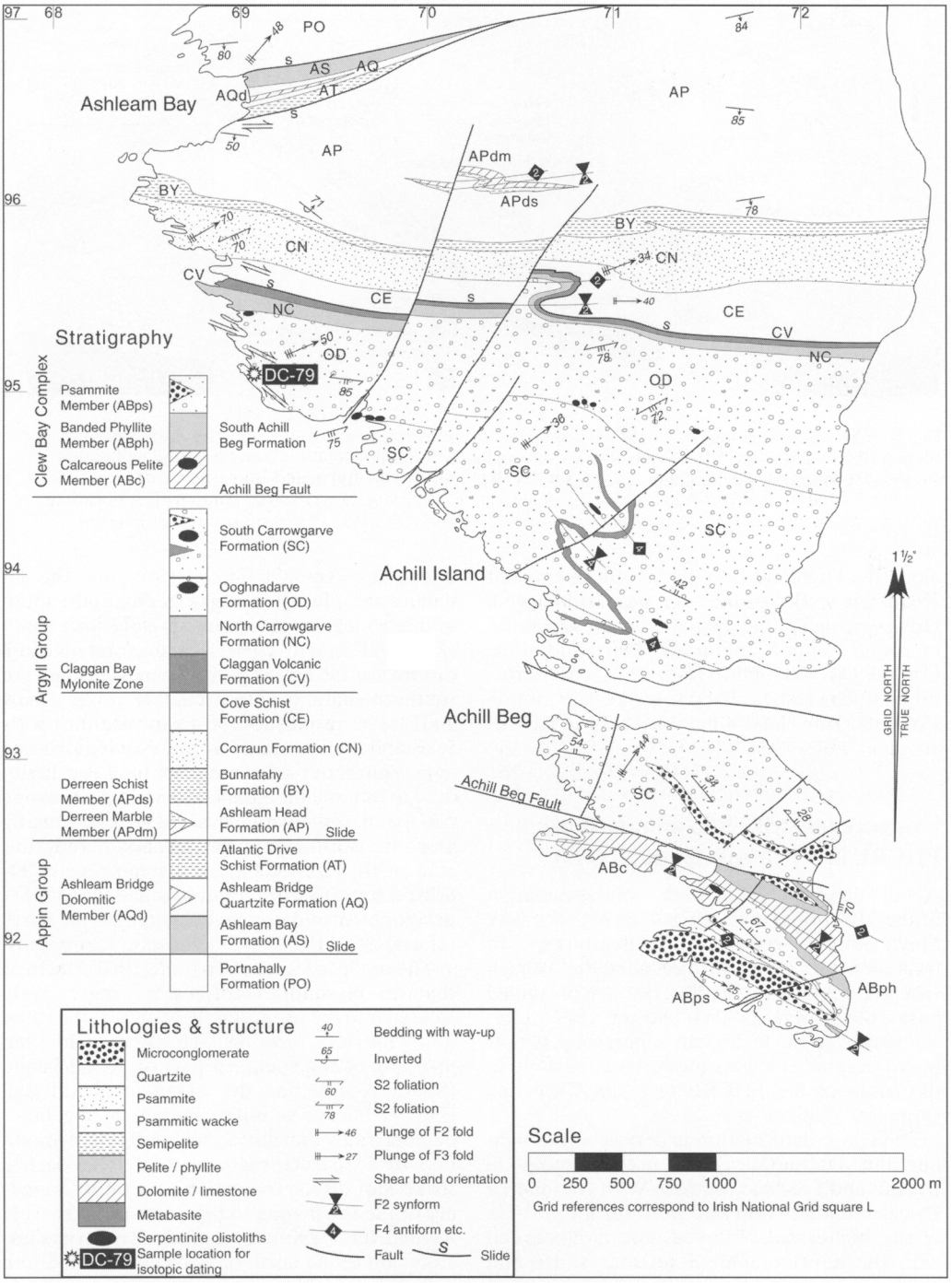

Fig. 3. Geological map of South Achill and Achill Beg.

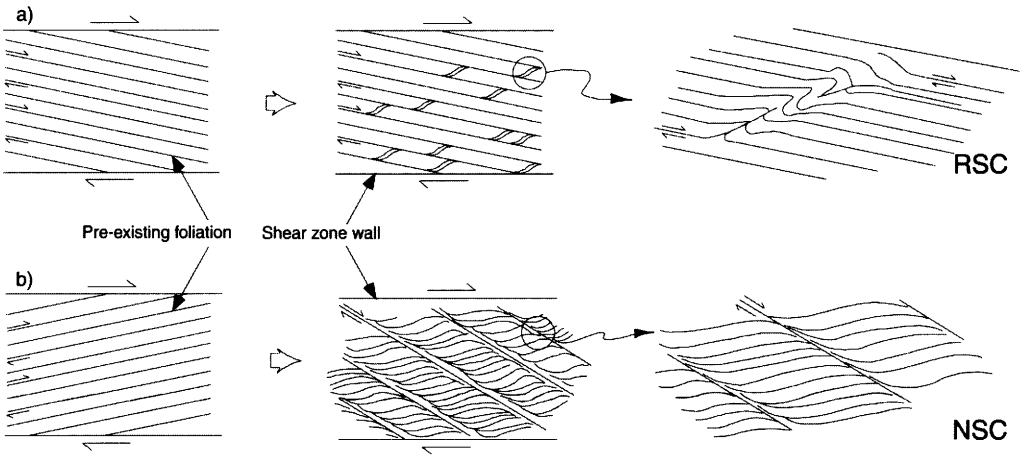

Fig. 4. Angular relationships predicted between the shear zone wall and the foliation-slip and crenulation-slip surfaces. (**a**) Reverse-slip crenulations. (**b**) Normal-slip crenulations. Reprinted from *Journal of Structural Geology*, **9**, Dennis & Secor: A model for the development of crenulations in shear zones with applications from the southern Appalachian Piedmont, pp. 809–817. Copyright 1987, with permission from Elsevier.

Crenulation-slip morphologies produced by oblique foliation-slip

The kinematic models of Dennis & Secor (1987, 1990) predict the crenulation morphologies that develop in order to compensate for the displacement component of foliation slip normal to the shear zone wall. In a dextral shear zone, when the pre-existing foliation is at an acute, clockwise angle to the shear zone wall (Fig. 4a), movement away from the shear zone wall due to oblique foliation slip is compensated by reverse-slip crenulations (RSC), which transfer slip up to 'higher' foliation planes. When the slipping foliation is at an acute anticlockwise angle to the shear zone wall in a dextral shear zone (Fig. 4b), movement normal to the shear zone wall is compensated by normal-slip crenulations (NSC).

Asymmetrical buckle folds (reverse-slip crenulations)

The most common crenulation-slip morphologies in South Achill and Achill Beg are asymmetrical buckle folds (Fig. 5a). The strike of the F_3 axial planes makes an angle of approximately 27° with the strike of the S_2 foliation in an anticlockwise direction (Fig. 6a). F_3 fold axes plunge moderately to the NE (Figs 3, 6a). The largest F_3 folds have wavelengths of only a few metres, and typically the smaller F_3 folds can be observed to 'root' in the S_2 foliation surface. These features are typical of the reverse-slip crenulations of Dennis & Secor (1987). With progressive dextral shear, the S_3 foliation which initiates anticlockwise to S_2 is progressively brought into parallelism (Fig. 5a). This is particularly evident where there is a large competence contrast across a bedding surface. Relatively rigid psammitic layers respond to D_3 shear by folding with S_3 usually oblique to S_2. If the S_3 foliation continues out into an adjacent graphitic pelite layer, then commonly the S_3 foliation swings clockwise into parallelism with S_2 and hence the weak graphitic pelite layers are accommodating the bulk of the displacement. The weak graphitic pelite layers also often display evidence of slip along the S_2 foliation surfaces (Fig. 5b). On a vertical surface, the S_3 foliation commonly rotates into the vertical parallel to S_2, with a down-to-the-south shear sense.

Extensional crenulation cleavages (normal-slip crenulations)

Extensional crenulation cleavages (Platt & Vissers 1980) are relatively common within pelitic lithologies in the South Achill sequence. They make an angle of approximately 29° (Fig. 6b) with the S_2 foliation in a clockwise direction, and consistently give a dextral sense of shear (Fig. 5c). Identical in style to the normal-slip crenulations of Dennis & Secor (1987), they are believed to be broadly contemporaneous with the F_3 asymmetrical buckle folds based on the absence of apparent overprinting relationships. The orientation of the earlier S_2 foliation controls the morphology of the later crenulations

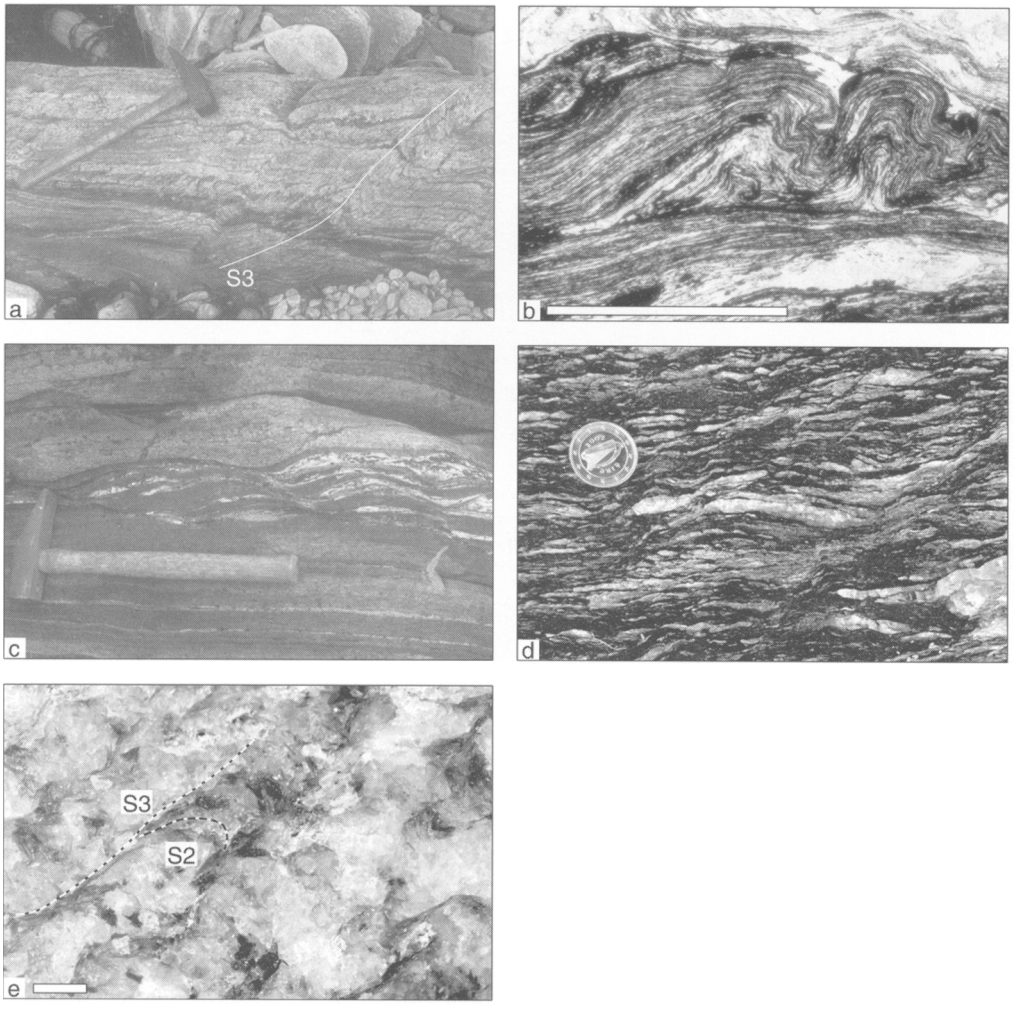

Fig. 5. (**a**) Asymmetrical buckle folds (F_3), interpreted as reverse slip crenulations (RSC). Later rotation of S_3 cleavage is due to progressive dextral shear. Hammer 40 cm long. South Achill Dalradian [L69329495]. (**b**) Graphitic pelite illustrating décollement-like slip along the S_2 foliation surface. Plane-polarized light, scale bar 1000 μm. South Achill Dalradian [L69039540]. (**c**) D_3 dextral shear bands cutting the S_2 foliation, interpreted as normal slip crenulations (NSC). Hammer 40 cm long. South Achill Dalradian [L69029544]. (**d**) Sinistral extensional crenulations affecting the composite S_2/S_3 foliation, interpreted as normal slip crenulations (NSC). Coin 2.2 cm in diameter. Central Ox Mountains Dalradian [G323026]. (**e**) Photograph of a polished rock slice used for ^{40}Ar–^{39}Ar *in situ* laserprobe dating of muscovite defining both the S_2 and S_3 foliations. Sample DC-79, scale bar 1000 μm. South Achill Dalradian [L69089511].

(e.g. RSC vs. NSC). On a vertical surface, the extensional shear bands give a down-to-the-south shear sense.

Orientation of the D_3 dextral shear zone

From the angular relationships proposed by Dennis & Secor (1987), the shear zone wall is expected to lie between the axial planes of the asymmetrical buckle folds (Fig. 6a) and the extensional shear bands (Fig. 6b). At localities which display both RSC and NSC fabrics, the dominant slip foliation (S_2) modified by the RSC makes a very small clockwise angle with the S_2 foliation affected by the NSC, similar to the geometry predicted by Fig. 4. However, on a

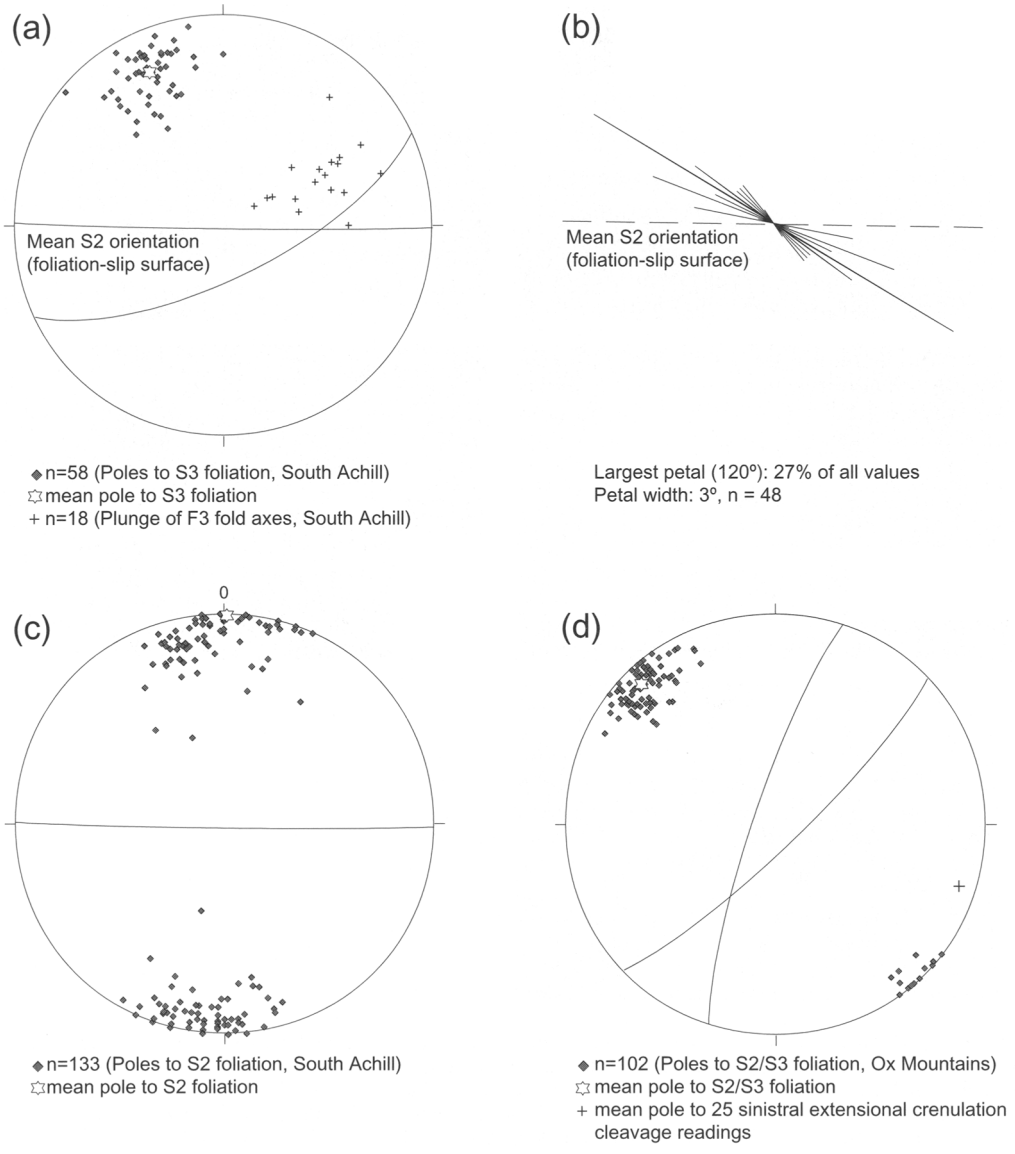

Fig. 6. (**a**) Stereographic plot of the orientation of RSC-related structures in South Achill (F_3 fold hinges and poles to the S_3 foliation) along with the mean orientation of the S_2 foliation. (**b**) Rose diagram illustrating the mean orientation of NSC-related structures in South Achill (dextral shears measured on horizontal surfaces). The mean orientation of the S_2 foliation is also illustrated. (**c**) Stereographic plot of the orientation of the pre-existing foliation-slip surface in South Achill (poles to the S_2 foliation). (**d**) Stereographic plot of the orientation of the pre-existing foliation-slip surface in the Central Ox Mountains (poles to the composite S_2/S_3 foliation), along with the mean orientation of NSC-related structures (sinistral extensional crenulation cleavages).

regional scale this relationship is not apparent and hence the dominant slip foliation (S_2) data for both the RSC and NSC sets are presented together (Fig. 6c). Combining data from both horizontal and vertical surfaces, the shear zone would therefore be an approximately east–west trending, sub-vertical structure, similar to the geometry proposed by Sanderson *et al.* (1980). No L_3 elongation lineations have been observed and hence although shear sense has been

determined reliably from the crenulation-slip morphologies on both horizontal and vertical surfaces, the exact shear direction remains uncertain.

Evidence for strike–slip motion along the FHCBL in the Central Ox Mountains

The Central Ox Mountains inlier consists of a sequence of Dalradian metasediments (Long & Max 1977; Alsop & Jones 1991) intruded by a Caledonian granite, the Ox Mountains granodiorite (Fig. 2a, c). The intrusion age of the Ox Mountain granodiorite has proved controversial in the past (e.g. Kennan 1997), and it is discussed in detail later. This granodiorite is intruded into the core of a significant upright D_3 antiform which trends NE–SW, subparallel to the length of the inlier (Fig. 2c; Taylor 1969). High strain zones are well developed on the limbs of the main D_3 antiformal structure, are parallel to the vertical, axial planar S_3 fabric and kinematic indicators such as rotated porphyroblasts and extensional crenulation cleavages display abundant evidence for sinistral shear (e.g. Hutton & Dewey 1986; Hutton 1987; Jones 1989; McCaffrey 1992, 1994). These shear zones have been regarded as contemporaneous with the development of the main D_3 antiform and the Central Ox Mountains has thus been regarded a transpressive sinistral shear zone during D_3 (Hutton & Dewey 1986; Hutton 1987; Jones 1989; McCaffrey 1992, 1994).

The Ox Mountains granodiorite itself also displays abundant evidence of sinistral strike–slip deformation. The main solid-state foliation is subvertical, strikes NE–SW and is accompanied by a stretching lineation which plunges gently to the NE or SW (McCaffrey 1992, 1994). NNE trending sinistral S–C fabrics are commonly well developed within the granodiorite and are subparallel to the asymmetrical extensional crenulation cleavages developed in the country rock (Hutton & Dewey 1986; McCaffrey 1992, 1994). The Ox Mountains granodiorite has thus been regarded as being emplaced synkinematically with respect to D_3 sinistral transpressive deformation in the country rock (Hutton & Dewey 1986; Jones 1989; McCaffrey 1992, 1994).

High strain zones (tectonic slides) in the Central Ox Mountains

Three high strain zones are particularly well developed on the SE flank of the Central Ox Mountains inlier – the Lough Talt Slide, the Glennawoo Slide and the Callow Shear Zone (Taylor 1969). In the Callow Loughs region (Fig. 7), the Lough Talt and Glennawoo Slides may be adequately represented as discrete shear zones, but the Callow Shear Zone is significantly wider (more than 750 m across strike) and is regarded as a substantial mylonite belt. Both the Glennawoo Slide and the Callow Shear Zone display abundant evidence of sinistral extensional crenulation cleavage development (Fig. 7).

Extensional crenulation cleavages (normal-slip crenulations)

In the Callow Loughs region, the main foliation is close to the vertical and trends NE (Figs 6d & 7). It is regarded as a composite S_2/S_3 fabric as S_2 and S_3 are usually coplanar (Jones 1989; MacDermot *et al.* 1996) and the S_3 fabric can only be conclusively identified when F_3 folds are present. F_3 folds plunge gently to the NE and verge towards the Ox Mountains granodiorite (Fig. 7). Extensional crenulation cleavages make an angle of approximately 28° (Fig. 6d) with the main (composite S_2/S_3 foliation) in an anticlockwise direction, and consistently give a sinistral sense of shear (Fig. 5d). On a vertical surface, the extensional shear bands give a down to the south shear sense.

The composite (S_2/S_3) main foliation is usually defined by muscovite, chlorite and equigranular quartz grains with interlobate grain boundaries. These quartz grains are typically of the order of 100–200 μm in diameter and display undulose extinction. MP3 porphyroblasts of albite and almandine garnet overgrow the main foliation and staurolite is locally developed (MacDermot *et al.* 1996). Along the extensional crenulation cleavage planes, quartz has undergone significant dynamic recrystallization. It is conspicuously finer grained (10–20 μm) than that defining the composite S_2/S_3 foliation, and has a weak shape-preferred orientation (aspect ratios of up to 3:1). Additionally, phyllosilicates within the shear bands (chlorite and muscovite) are significantly finer grained than those defining the S_2/S_3 foliation. The extensional crenulation cleavage planes are short and anastomosing, commonly rooting in the pre-existing composite S_2/S_3 foliation, and are very similar in morphology to the normal-slip crenulations (NSC) of Dennis & Secor (1987).

Isotopic dating of crenulation-slip surfaces

Many deformed rocks contain evidence (e.g. multiple fabrics) for having experienced more

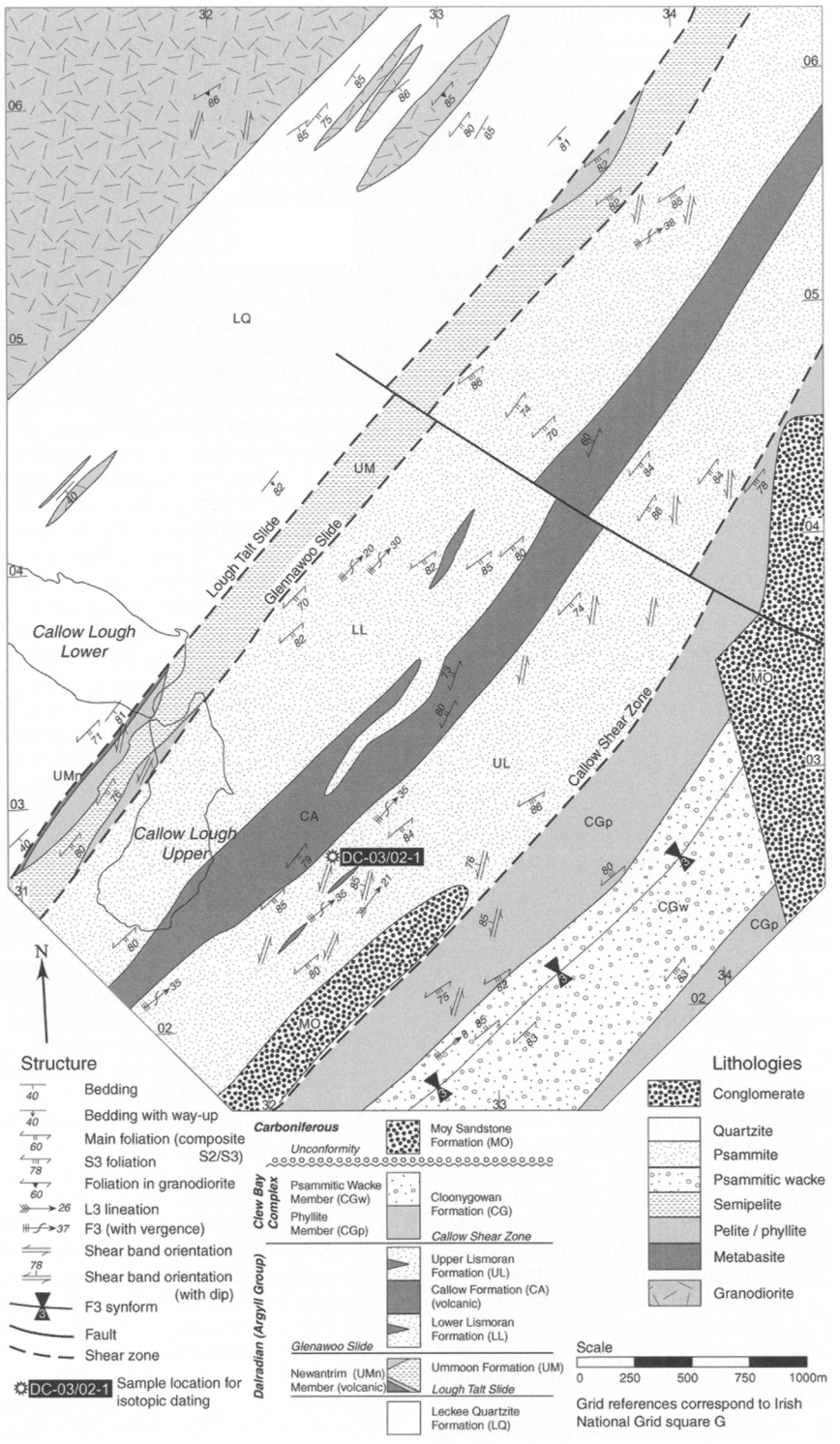

Fig. 7. Geological map of the Callow Loughs area in the Central Ox Mountains.

than one deformation event. The timing of growth of multiple fabrics can be constrained by dating fabric-forming minerals which crystallize below their closure temperatures (e.g. Cliff 1985). One of the most common fabric-forming minerals is muscovite, and Rb–Sr dating and ^{40}Ar–^{39}Ar laserprobe dating of multiple generations of muscovite has been employed in many studies (e.g. Müller *et al.* 1999).

Both the Rb–Sr and Ar–Ar systems have shown that muscovite grown below its closure temperature during deformation (e.g. in mylonites) may record the age of neocrystallization (e.g. Dunlap 1997; Freeman *et al.* 1997, Müller *et al.* 1999). Additionally, samples containing earlier generations of white mica (e.g. as porphyroclasts or older foliations) record the crystallization age of these early fabrics where they have not been rejuvenated by later deformation (West & Lux 1993; Freeman *et al.* 1997, Müller *et al.* 1999).

In this study, fabric-forming muscovite has been dated using the ^{40}Ar–^{39}Ar and Rb–Sr systems in order to constrain both the age of shearing and the age of the reactivated foliation-slip surface within samples that have undergone shear-related deformation along the FHCBL. The age of the pre-existing foliation which is exploited by shearing along the FHCBL is also well constrained by previous geochronological studies based immediately outside of this shear zone (e.g. Flowerdew *et al.* 2000; Chew *et al.* 2003), where it is unaffected by later deformation. Thus the age of this foliation in undeformed samples and in samples where it has been reactivated due to subsequent shearing can be compared.

Pre-existing constraints on the age of the foliation-slip fabric in both inliers

Recent geochronological studies in the Dalradian of NW Ireland (Flowerdew *et al.* 2000; Chew *et al.* 2003) has shown that main foliation development in both South Achill and the Central Ox Mountains inlier is Grampian (*c.* 470–460 Ma) in age in samples which are unaffected by later shearing along the FHCBL. Knowledge of the age of this main foliation in samples unaffected by later deformation is essential, as it enables us to assess whether the age of the reactivated foliation is partially reset when it is rejuvenated by later shearing along the FHCBL.

Four Rb–Sr S_2 muscovite ages from the Dalradian of South Achill range from 460–458 Ma (± 7 Ma), and four ^{40}Ar–^{39}Ar S_2 muscovite step-heating plateaux from the same samples range from 463–457 Ma (± 4 Ma) (Chew *et al.* 2003). Two Rb–Sr S_2 muscovite ages of 460 ± 7 Ma and 461 ± 7 Ma have been obtained from the low greenschist facies Clew Bay Complex and probably record crystallization (Chew *et al.* 2003). As this outboard terrane (Figs 2 & 3) is in structural continuity with the Dalradian Supergroup (Chew 2003), it is thought likely that the *c.* 460 Ma Rb–Sr S_2 muscovite ages for the South Achill Dalradian also record crystallization during the Grampian orogeny, particularly as the peak metamorphic temperature in South Achill is unlikely to have exceeded 450 °C (Chew *et al.* 2003). The marked similarity with the S_2 muscovite ^{40}Ar–^{39}Ar step heating data may imply that the Ar–Ar system is recording either rapid cooling or crystallization, despite growing *c.* 50 to 100 °C above its closure temperature (*c.* 350–400 °C; Wijbrans & McDougall 1988). The possibility of extraneous Ar contamination is discussed in detail later.

One ^{40}Ar–^{39}Ar hornblende age of 467 ± 3 Ma and one Rb–Sr muscovite age of 472 ± 8 Ma have been obtained from the composite S_2/S_3 foliation in the Dalradian of Central Ox Mountains inlier (Flowerdew *et al.* 2000). Younger ^{40}Ar–^{39}Ar and Rb–Sr ages (429–410 Ma) have been strongly influenced by the intrusion of the Ox Mountains granodiorite. Similar Grampian (*c.* 470–460) ages have also been obtained from Dalradian rocks in the NE Ox Mountains (Fig. 1). Here Dalradian rocks are interleaved during D_3 with the Slishwood Division, a unit of psammitic gneisses which has experienced late Precambrian granulite-facies metamorphism (Sanders *et al.* 1987). Three ^{40}Ar–^{39}Ar hornblende ages and six Rb–Sr muscovite ages defining the S_3 foliation within the interleaved Dalradian range from 470–446 Ma. The older S_3 mineral ages are indistinguishable from the older ages (472 ± 7 Ma, 467 ± 3 Ma) obtained from the composite S_2/S_3 fabric in the Central Ox Mountains inlier (Flowerdew *et al.* 2000).

Sampling

In this study we present isotopic data from two Dalradian samples from two localities. DC-79 is a semipelite from South Achill (Fig. 3) in which muscovite defining both the local S_2 and S_3 foliations was dated *in situ* by the ^{40}Ar–^{39}Ar laserprobe spot fusion method. DC-03/02–1 is a semipelite from the Central Ox mountains inlier (Fig. 7) from which a bulk mineral separate of muscovite defining the main (composite S_2/S_3) foliation was analysed by the Rb–Sr method. The whole rock was also analysed.

Table 1. *^{40}Ar–^{39}Ar spot fusion data*

Spot	Laser power	^{36}Ar(a)	^{37}Ar(Ca)	^{38}Ar(Cl)	^{39}Ar(K)	^{40}Ar(r)	Age (Ma)	± 2σ	^{40}Ar(r) (%)	^{39}Ar(k) (%)
Sample DC-79, S_2 and S_3 ms. Dalradian, South Achill (L69089511).										
2 (S_2)	Fusion	0.0002	0.0000	0.0001	0.1262	9.0407	453.4	3.4	99.2	7.1
4 (S_2)	Fusion	0.0002	0.0266	0.0000	0.0320	2.2206	441.3	10.1	97.3	1.8
6 (S_2)	Fusion	0.0000	0.0299	0.0002	0.0209	1.5135	457.8	14.5	99.4	1.2
10 (S_2)	Fusion	0.0010	0.0208	0.0000	0.5635	40.1131	450.7	1.3	99.3	31.7
11 (S_2)	Fusion	0.0004	0.0308	0.0004	0.1893	13.5803	453.8	3.5	99.1	10.7
1 (S_3)	Fusion	0.0001	0.0000	0.0000	0.1492	10.5535	448.2	2.8	99.7	8.4
3 (S_3)	Fusion	0.0000	0.0000	0.0001	0.0972	6.8772	448.2	3.5	99.8	5.5
5 (S_3)	Fusion	0.0001	0.0345	0.0001	0.1325	9.3329	446.6	3.6	99.8	7.5
7 (S_3)	Fusion	0.0013	0.0511	0.0002	0.0683	4.7528	441.7	5.5	92.4	3.8
8 (S_3)	Fusion	0.0002	0.0371	0.0000	0.0891	6.2796	446.9	4.8	99.0	5.0
9 (S_3)	Fusion	0.0003	0.0178	0.0000	0.3099	22.0392	450.4	1.9	99.6	17.4
Weighted average* (S_2 spots): 451 ± 2 Ma (2σ)										
Weighted average (S_3 spots): 448 ± 3 Ma (2σ)										
J value: 0.003987 ± 0.5% (1σ)										

*Weighted averages calculated using ISOPLOT (Ludwig 1999) and use the 2σ error associated with each analysis.

Analytical methods

^{40}Ar–^{39}Ar spot fusion analyses were carried out using the VULKAAN argon laserprobe (Wijbrans *et al.* 1995) at the Vrije Universiteit in Amsterdam. Samples were irradiated at the HPPIF facility in the high flux research reactor at Petten, Netherlands. Polished slices were interspersed between the Al tablets containing the flux monitor DRA-1 sanidine (24.99 ± 0.07 Ma; Wijbrans *et al.* 1995) prior to irradiation. Four flux monitors were used to construct a J-curve with a 0.5% error (1σ). Samples were analysed within six months of irradiation to minimize the interference effects produced by radioactive decay after irradiation. The analytical procedure is described in detail by Wijbrans *et al.* (1995) and is outlined below. Samples were heated using a continuous 18 W argon ion laser (454.5–514.5 nm wavelength). For spot fusion experiments, several short laser pulses (0.1 s) excavated a pit approximately 30 microns in diameter, surrounded by a crater of melt material. The Ar released was cleaned with Fe–V–Zr getters (250 °C), prior to analysis on a MAP-215/50 mass spectrometer. Data reduction was carried out using in-house software, ArArCALC V20. Blank intensities were measured every 3–5 sample runs and mass fractionation was corrected for by regular measurement of shots of clean air argon.

For Rb–Sr analyses, standard ion exchange methods were used for chemical separation of elements. Samples were loaded on tantalum filaments and were analysed on a semi-automated single collector VG Micromass 30 mass spectrometer at the Department of Geology, University College Dublin. During the course of analysis, NBS SRM 987 gave $^{87}Sr/^{86}Sr$ ratios of 0.71027 ± 5 (n = 8, 2σ) and NBS SRM 607 yielded $^{87}Rb/^{86}Sr$ ratios of 8.005 ± 13 (n = 7, 2σ). Sr blanks averaged 1.5 ng and are not significant. 2σ analytical uncertainties of 1.5% for $^{87}Rb/^{86}Sr$ and tabulated values (Table 2) for $^{87}Sr/^{86}Sr$ ratios were used in age calculations which employed a value of 0.0142 Ga^{-1} for the ^{87}Rb decay constant (Steiger and Jäger 1977).

Constraining dextral shear in NW Mayo (South Achill)

New S_3 mica growth is not commonly associated with the D_3 deformation event in South Achill, but locally S_3 muscovite is found overgrowing a crenulated S_2 fabric in the hinges of asymmetrical buckle folds (reverse-slip crenulations associated with D_3 dextral shear). One polished slice from the hinge of an F_3 fold was selected for *in situ* ^{40}Ar–^{39}Ar laserprobe spot fusion analyses (Table 1). Sample DC-79 is semipelitic, with an S_2 foliation defined by muscovite and minor chlorite and epidote. Individual muscovite grains are typically around 500 μm long and 50 μm wide, but both the S_2 and S_3 fabrics are composed of seams of white mica which are typically several grains in width. Typically S_3 seams are approximately 150 μm across (Fig. 5e), whereas S_2 lithons are larger and may be up to 500 μm wide (Fig. 5e). Chlorite grains are

typically similar in size to the muscovite grains (*c.* 500 μm long and 50 μm wide) and the largest epidote needles observed are 200 μm long. The S_2 foliation is overgrown by MP2 plagioclase which is augened by the seams of S_3 muscovite. The calcic component in some of the Ar analyses (Table 1) is probably derived from the epidote, as the MP2 plagioclase is essentially pure albite. Muscovite defining the S_2 foliation is typically more celadonite-rich and paragonite-poor than the later (S_3) fabric (Chew *et al.* 2003).

In situ ^{40}Ar–^{39}Ar laserprobe dating of the S_3 muscovite seams yields a weighted mean age of 448 ± 3 Ma, whereas the older, crenulated S_2 muscovite seams yield a weighted mean age of 451 ± 2 Ma (Table 1). The ^{40}Ar–^{39}Ar system is only reliably recording the youngest deformation fabrics present, as undeformed S_2 muscovite from South Achill yields consistent *c.* 460 Ma Rb–Sr and ^{40}Ar–^{39}Ar ages (Chew *et al.* 2003). The 448 ± 3 Ma age for muscovite within the S_3 crenulation-slip fabric is interpreted as a crystallization age based on the low-greenschist facies assemblages observed in the S_3 crenulation seams as detailed above.

The possibility of extraneous argon cannot be ruled out, particularly in a high-pressure, low temperature terrane such as South Achill. Excess argon (argon with $^{40}Ar/^{36}Ar$ ratios which differ from the modern atmospheric ratio of 295.5) has been documented in white mica from several high-pressure, low-temperature terranes (e.g. Arnaud & Kelley 1995; Sherlock & Kelley 2002). The presence of excess argon may be evaluated by using an inverse isochron correlation diagram (a plot of $^{36}Ar/^{40}Ar$ versus $^{39}Ar/^{40}Ar$) as the incorporation of excess argon will result in the intercept of the isochron on the ordinate axis deviating from the modern atmospheric $^{40}Ar/^{36}Ar$ ratio of 295.5. However, K-rich phases (such as white mica) can produce large quantities of radiogenic ^{40}Ar, and hence the data often cluster close to the $^{39}Ar/^{40}Ar$ axis. The presence of excess argon is therefore difficult to assess, as the intercept with the $^{36}Ar/^{40}Ar$ axis is poorly constrained. This is the case with the South Achill Ar data. The presence of excess argon has also been documented in samples which yield intercepts within error of the modern $^{40}Ar/^{36}Ar$ atmospheric ratio on an inverse isochron correlation diagram (Sherlock & Arnaud 1999).

Studies that have documented the presence of excess argon in white mica in high-temperature, low-pressure terranes instead are based on ^{40}Ar–^{39}Ar phengite ages that are significantly older than either the corresponding Rb–Sr phengite ages or other geochronometers with significantly higher closure temperatures (e.g. Arnaud & Kelley 1995; Sherlock & Arnaud 1999). This disparity is not observed in South Achill as both the Rb–Sr and ^{40}Ar–^{39}Ar ages for undeformed S_2 muscovite ages cluster at *c.* 460 Ma (Chew *et al.* 2003) and are mutually within error. The S_3 muscovite ages are temporally distinct, and are clearly post-Grampian (*c.* 470–460 Ma) in age.

Constraining sinistral shear in the Central Ox Mountains

The Central Ox Mountains displays extensional crenulation cleavage development superimposed on what is believed to be a pre-existing Grampian (S_2/S_3) foliation. However, whereas dextral shear in South Achill was constrained by dating both the pre-existing foliation-slip surface and the later crenulation-slip surfaces within the same sample, this strategy has proved impossible in the Central Ox Mountains. Dalradian metasediments in the Central Ox Mountains display only limited growth of extremely fine-grained muscovite on extensional crenulation cleavage surfaces, which is not sufficient for isotopic dating. However, pegmatites and granite sheets associated with the Ox Mountains granodiorite are intruded into the Dalradian metasediments, and in common with the Ox Mountains granodiorite, the pegmatites and granite sheets were emplaced synkinematically with respect to sinistral deformation in the country rocks (McCaffrey 1992, 1994). Sinistral shearing in the Central Ox Mountains can thus be constrained by dating pegmatite crystallization. The age of the foliation surface that is affected by sinistral extensional crenulation cleavages in the Central Ox Mountains has until now remained uncertain, as previous geochronological studies in the inlier (e.g. Flowerdew *et al.* 2000) were undertaken on foliated samples that were not affected by later deformation. Whereas the reactivated foliation surface is believed to be the regional S_2/S_3 composite foliation based on detailed field mapping (Fig. 7), it may have developed contemporaneously with sinistral shear development in the Central Ox Mountains, as the timing relationship between mylonitic foliation development and cross-cutting shear bands can be often difficult to establish (e.g. Lister & Snoke 1984).

The age of the pre-existing foliation has been constrained by a Rb–Sr muscovite–whole rock age from a semi-pelitic schist sample displaying a pervasive sinistral extensional crenulation cleavage (Fig. 5d). This age of 448 ± 9 Ma (Table 2) is

Table 2. *Rb–Sr geochronology*

Sample	Locality and Irish National Grid Ref.	Textural relationship	Mineral	Rb(ppm)	Sr(ppm)	$^{87}Rb/^{86}Sr$	$^{87}Sr/^{86}Sr \pm 2\sigma$	$^{87}Sr/^{86}Sr(i)$	Age ± 2σ (Ma)
DC-03/02–131	Lismoran (G323026)	Main foliation (composite S_2/S_3)	muscovite	338.77	126.60	7.79	0.776157 ± 56	0.72641	448 ± 9
			whole rock	77.8571	141.07	1.60	0.736629 ± 58		

Table 3. *Rb–Sr geochronology of Ox Mountains pegmatites from Flowerdew* et al. *(2000)*

Sample	Irish National Grid Ref.	Sample description	Minerals dated	Age ± 2σ (Ma)
37	G270003	Dalradian-hosted pegmatite	coarse igneous muscovite–K feldspar	392 ± 6
38	M167963	Dalradian-hosted pegmatite	coarse igneous muscovite–plagioclase	400 ± 6
39	G198956	Dalradian-hosted pegmatite	coarse igneous muscovite–K feldspar	402 ± 6
40	G242069	Ox Mountains granodiorite	coarse igneous muscovite–K feldspar	400 ± 6
37	G270003	Dalradian-hosted pegmatite	recrystallized muscovite–K feldspar	381 ± 6
40	G242069	Ox Mountains granodiorite	recrystallized muscovite–K feldspar	384 ± 6
41	G198956	Dalradian-hosted pegmatite	recrystallized muscovite–plagioclase	384 ± 5

slightly younger than the *c.* 470–460 Ma age estimates for the Grampian S_3 foliation in the Central and NE Ox Mountains inliers (Flowerdew *et al.* 2000). However, it is broadly coincident with most of the mineral cooling age data from the Central and NE Ox Mountains inliers which cluster at or around 460–450 Ma (Flowerdew *et al.* 2000), and the reactivated foliation surface is thus thought to represent the regional composite Grampian S_2/S_3 foliation.

The pre-existing foliation surface is markedly older than the age constraints for sinistral extensional crenulation cleavage development in the Central Ox Mountains inlier. Sinistral shearing is constrained by four Rb–Sr muscovite–feldspar ages from pegmatites which range from 402–392 Ma (Table 3) which are interpreted as recording igneous crystallization (Flowerdew *et al.* 2000). Late sinistral shearing has recrystallized coarse magmatic muscovite within both the Ox Mountains pegmatite suite and the Ox Mountains granodiorite, yielding three Rb–Sr muscovite–feldspar ages of between 385 and 381 Ma (Table 3; Flowerdew *et al.* 2000).

Discussion on the intrusion age of the Ox Mountains granodiorite

Sinistral shearing along the FHCBL in the Central Ox Mountains is effectively constrained by the age of intrusion of the Ox Mountains granodiorite and its presumed coeval pegmatite suite. However, in contrast to the *c.* 400 Ma age obtained from the Ox Mountains pegmatite suite (see above), the Ox Mountains granodiorite has yielded *c.* 480 Ma Rb–Sr whole rock isochrons (Pankhurst *et al.* 1976; Max *et al.* 1976). The old Rb–Sr ages suggest that granite emplacement and therefore sinistral strike–slip deformation occurred either before or very early in the Grampian orogeny.

However several lines of evidence mitigate against a *c.* 480 Ma intrusion age. Most of the Ox Mountains granodiorite Rb–Sr whole rock data are characterized by low $^{87}Rb/^{86}Sr$ values, typically less than 2. Rb–Sr whole rock isochrons characterized by low $^{87}Rb/^{86}Sr$ values have also been obtained from other Caledonian granites, and these too yield *c.* 480 Ma intrusion ages even though the intrusion is demonstrably younger (*c.* 400 Ma) by independent evidence (Kennan 1997). Additionally, unpublished U–Pb multigrain zircon data suggest a *c.* 415 Ma intrusion age for the Ox Mountains granodiorite (MacDermot *et al.*, 1996). This is consistent with the youngest mineral cooling ages (*c.* 410 Ma) obtained from the Central Ox Mountains inlier close to the Ox Mountains granodiorite which are likely to be due to thermal resetting, and a *c.* 400 Ma emplacement age for the pegmatite suite (Flowerdew *et al.* 2000); a *c.* 400 Ma intrusion age for the Ox Mountains granodiorite is more likely.

Earlier movements along the FHCBL

This study documents two examples of post-Grampian strike–slip movement along the

FHCBL. However, there is evidence for earlier stages of movement along the FHCBL during the Grampian orogeny, illustrating further how this important crustal-scale shear zone has had a long and complicated history of movement. In Tyrone, the D_3 Omagh Thrust has translated inverted Dalradian rocks towards the ESE (Fig. 1) over Arenig–Llanvirn shales of the Tyrone volcanics (Alsop & Hutton 1993). In southern Donegal and the NE Ox Mountains inlier, Dalradian rocks were thrust to the SE over granulite-facies basement of the Slishwood Division (Fig. 1) along the Lough Derg Slide (Alsop 1991) and the North Ox Mountains Slide (Flowerdew 1998/9) respectively. Tectonic juxtaposition (D_3) of the Dalradian and Slishwood Division is likely to have occurred between 470 and 460 Ma based on ^{40}Ar–^{39}Ar, Rb–Sr and Sm–Nd mineral ages (Flowerdew *et al.* 2000). Thus in Donegal, the NE Ox Mountains and Tyrone, the earliest constrained phase of movement (*c.* 470–460 Ma) along the Fair Head–Clew Bay Line involves the translation of the main Dalradian nappes over outboard terranes to the SE.

Conclusions

The Fair Head–Clew Bay Line has been shown to have been reactivated several times. It was originally active as a ductile thrust during the (*c.* 470–460 Ma) Grampian orogeny, where Dalradian nappes adjacent to the Fair Head–Clew Bay Line were thrust over outboard terranes to the SE.

The Dalradian metasediments have undergone two separate phases of post-Grampian strike–slip movement adjacent to the Fair Head–Clew Bay Line. These two phases of movement have produced reverse-slip and normal-slip crenulations which modified the earlier Grampian nappe fabrics, and tilted the initially recumbent Grampian nappes into a vertical orientation (Fig. 2b, c).

The development of the reverse-slip and normal-slip crenulations produced by these two discrete phases of strike–slip movement has been constrained by isotopic dating. Dextral displacement along the Fair Head–Clew Bay Line in the NW Mayo inlier is constrained to *c.* 448 Ma, whereas sinistral displacement along the Fair Head–Clew Bay Line in the Ox Mountains inlier is constrained to *c.* 400 Ma based on previously published pegmatite intrusion ages.

Major crustal-scale shear zones may therefore have a long and complicated history of movement, in which pre-existing planar anisotropies (e.g. foliations) act as slip surfaces during later non-coaxial deformation. Careful analysis of the resulting crenulation morphologies combined with isotopic dating yields a more complete understanding of the reactivation history of major crustal-scale shear zones.

D.M.C. gratefully acknowledges a Forbairt Basic Research Grant and a UCD Research Doctoral Scholarship. Barry Long is thanked for many fruitful discussions about Dalradian geology, and the Central Ox Mountains in particular. Sarah Sherlock and Grahame Oliver are thanked for their careful and constructive reviews, which significantly improved this paper.

References

ALSOP, G.I. 1991. Gravitational collapse and extension along a mid-crustal detachment: the Lough Derg Slide, northwest Ireland. *Geological Magazine*, **128**, 345–354.

ALSOP, G.I. & HUTTON, D.H.W. 1993. Major southeast-directed Caledonian thrusting and folding in the Dalradian rocks of mid-Ulster: implications for Caledonian tectonics and mid-crustal shear zones. *Geological Magazine*, **130**, 233–244.

ALSOP, G.I. & JONES, C.S. 1991. A review and correlation of Dalradian stratigraphy in the Ox Mountains and southern Donegal, Ireland. *Irish Journal of Earth Sciences*, **11**, 99–112.

ARNAUD, N.O. & KELLEY, S.P. 1995. Evidence for excess argon during high pressure metamorphism in the Dora Maira Massif (western Alps, Italy), using an ultraviolet laser ablation microprobe ^{40}Ar–^{39}Ar technique. *Contributions to Mineralogy and Petrology*, **121**, 1–11.

CHEW, D.M. 2003. Structural and stratigraphic relationships across the continuation of the Highland Boundary Fault in western Ireland. *Geological Magazine*, **140**, 73–85.

CHEW, D.M., DALY, J.S., PAGE, L.M. & KENNEDY, M.J. 2003. Grampian orogenesis and the development of blueschist-facies metamorphism in western Ireland. *Journal of the Geological Society, London*, **160**, 911–924.

CLIFF, R.A. 1985. Isotopic dating in metamorphic belts. *Journal of the Geological Society, London*, **142**, 97–110.

DALY, J.S. 1996. Pre-Caledonian history of the Annagh Gneiss Complex, north-western Ireland, and correlation with Laurentia–Baltica. *Irish Journal of Earth Sciences*, **15**, 5–18.

DENNIS, A.J. & SECOR, D.T. 1987. A model for the development of crenulations in shear zones with applications from the southern Appalachian Piedmont. *Journal of Structural Geology*, **9**, 809–817.

DENNIS, A.J. & SECOR, D.T. 1990. On resolving shear direction in foliated rocks deformed by simple shear. *Geological Society of America Bulletin*, **102**, 1257–1267.

DEWEY, J.F. & SHACKLETON, R.M. 1984. A model for the evolution of the Grampian tract in the early

Caledonides and Appalachians. *Nature*, **312**, 115–121.

DUNLAP, W.J. 1997. Neocrystallization or cooling? $^{40}Ar/^{39}Ar$ ages of white micas from low-grade mylonites. *Chemical Geology*, **143**, 181–203.

FLOWERDEW, M.J. 1998/9. Tonalite bodies and basement–cover relationships in the North-eastern Ox Mountains Inlier, north-western Ireland. *Irish Journal of Earth Sciences*, **17**, 71–82.

FLOWERDEW, M.J., DALY, J.S., GUISE, P.G. & REX, D.C. 2000. Isotopic dating of overthrusting, collapse and related granitoid intrusion in the Grampian orogenic belt, northwestern Ireland. *Geological Magazine*, **137**, 419–435.

FREEMAN, S.R., INGER, S., BUTLER, R.W.H. & CLIFF, R.A. 1997. Dating deformation using Rb–Sr in white mica: greenschist facies deformation ages from the Entrelor shear zone, Italian Alps. *Tectonics*, **16**, 57–76.

FRIEDRICH, A.M., BOWRING, S.A., MARTIN, M.W. & HODGES, K.V. 1999*a*. Short-lived continental magmatic arc at Connemara, western Ireland Caledonides: implications for the age of the Grampian orogeny. *Geology*, **27**, 27–30.

FRIEDRICH, A.M., HODGES, K.V., BOWRING, S.A. & MARTIN, M.W. 1999*b*. Geochronological constraints on the magmatic, metamorphic and thermal evolution of the Connemara Caledonides, western Ireland. *Journal of the Geological Society, London*, **156**, 1217–1230.

HARRIS, D.H.M. 1993. The Caledonian evolution of the Laurentian margin in western Ireland. *Journal of the Geological Society, London*, **150**, 669–672.

HARRIS, D.H.M. 1995. Caledonian transpressional terrane accretion along the Laurentian margin in Co. Mayo, Ireland. *Journal of the Geological Society, London*, **152**, 797–806.

HUTTON, D.H.W. 1987. Strike-slip terranes and a model for the evolution of the British and Irish Caledonides. *Geological Magazine*, **124**, 405–425.

HUTTON, D.H.W. & DEWEY, J.F. 1986. Palaeozoic terrane accretion in the Irish Caledonides. *Tectonics*, **5**, 1115–1124.

JONES, C.S. 1989. The structure and kinematics of the Ox Mountains, western Ireland; a mid-crustal transcurrent shear-zone. Unpublished Ph.D. thesis, University of Durham.

KENNAN, P.S. 1997. Granite: a singular rock. *In*: *Occasional papers in Irish science and technology*, **15**. Royal Dublin Society, 16.

KENNEDY, M.J. 1980. Serpentinite-bearing mélange in the Dalradian of County Mayo and its significance in the development of the Dalradian basin. *Journal of Earth Sciences of the Royal Dublin Society*, **3**, 117–126.

LISTER, G.S. & SNOKE, A.W. 1984. S-C mylonites. *Journal of Structural Geology*, **6**, 617–638.

LONG, C.B. & MAX, M.D. 1977. Metamorphic rocks in the SW Ox Mountains Inlier, Ireland; their structural compartmentation and place in the Caledonian orogen. *Journal of the Geological Society, London*, **133**, 413–432.

LUDWIG, K.R. 1999. Users Manual for Isoplot/Ex, Version 2.10: a geochronological toolkit for Microsoft Excel. *Berkeley Geochronology Center Special Publication*, **1a**, 49 pp.

MACDERMOT, C.V., LONG, C.B. & HARNEY, S. 1996. *Geology of Sligo-Leitrim: A geological description of Sligo, Leitrim, and adjoining parts of Cavan, Fermanagh, Mayo and Roscommon, to accompany the Bedrock Geology 1:100 000 Scale Map Series, Sheet 7, Sligo-Leitrim*. Geological Survey of Ireland.

MAX, M.D. & RIDDIHOUGH, R.P. 1975. Continuation of the Highland Boundary fault in Ireland. *Geology*, **3**, 206–210.

MAX, M.D., LONG, C.B. & SONET, J. 1976. The geological age and setting of the Ox Mountains Granodiorite. *Bulletin of the Geologial Survey of Ireland*, **2**, 27–5.

MCCAFFREY, K.J.W. 1992. Igneous emplacement in a transpressive shear zone: Ox Mountains igneous complex. *Journal of the Geological Society, London*, **149**, 221–235.

MCCAFFREY, K.J.W. 1994. Magmatic and solid state deformation partitioning in the Ox Mountains granodiorite. *Geological Magazine*, **131**, 639–652.

MÜLLER, W., DALLMEYER, R.D., NEUBAUER, F. & THONI, M. 1999. Deformation-induced resetting of Rb/Sr and $^{40}Ar/^{39}Ar$ mineral systems in a low-grade, polymetamorphic terrane (Eastern Alps, Austria). *Journal of the Geological Society, London*, **156**, 261–278.

PANKHURST, R.J., ANDREWS, J.R., PHILLIPS, W.E.A., SANDERS, I.S. & TAYLOR, W.E.G. 1976. Age and structural setting of the Slieve Gamph Igneous Complex, Co. Mayo, Ireland. *Journal of the Geological Society, London*, **132**, 327–36.

PLATT, J.P. & VISSERS, R.L. 1980. Extensional structures in anisotropic rocks. *Journal of Structural Geology*, **2**, 397–410.

RAMSAY, J.G. & GRAHAM, R.H. 1970. Strain variation in shear belts. *Canadian Journal of Earth Sciences*, **7**, 786–813.

RYAN, P.D., SOPER, N.J., SNYDER, D.B., ENGLAND, R.W. & HUTTON, D.H.W. 1995. The Antrim–Galway Line: a resolution of the Highland Border fault enigma of the Caledonides of Britain and Ireland. *Geological Magazine*, **132**, 171–184.

SANDERS, I.S., DALY, J.S. & DAVIES, G.R. 1987. Late Proterozoic high-pressure granulite facies metamorphism in the north-east Ox inlier, north-west Ireland. *Journal of Metamorphic Geology*, **5**, 69–85.

SANDERSON, D.J., ANDREWS, J.R., PHILLIPS, W.E.A. & HUTTON, D.H.W. 1980. Deformation studies in the Irish Caledonides. *Journal of the Geological Society, London*, **137**, 289–302.

SHERLOCK, S.C. & ARNAUD, N.O. 1999. Flat plateau and impossible isochrons: Apparent ^{40}Ar–^{39}Ar geochronology in a high-pressure terrain. *Geochimica et Cosmochimica Acta*, **63**, 2835–2838.

SHERLOCK, S.C. & KELLEY, S.P. 2002. Excess argon evolution in *HP–LT* rocks: a UVLAMP study of phengite and K-free minerals, NW Turkey. *Chemical Geology*, **182**, 619–636.

STEIGER, R.H. & JÄGER, E. 1977. Subcommission on geochronology: convention on the use of decay

constants in geo- and cosmochronology. *Earth and Planetary Science Letters*, **36**, 359–362.

TAYLOR, W.E.G. 1969. The structural geology of the Dalradian rocks of Slieve Gamph, Cos. Mayo and Sligo, western Ireland. *Geologische Rundschau*, **57**, 564–588.

WEST, D.P.W. & LUX, D.R. 1993. Dating mylonitc deformation by the ^{40}Ar–^{39}Ar method: an example from the Norumbega Fault Zone, Maine. *Earth and Planetary Science Letters*, **120**, 221–237.

WIJBRANS, J.R. & MCDOUGALL, I. 1988. Metamorphic evolution of the Attic Cycladic Metamorphic Belt on Naxos (Cyclades, Greece) utilizing $^{40}Ar/^{39}Ar$ age spectrum measurements. *Journal of Metamorphic Geology*, **6**, 571–594.

WIJBRANS, J.R., PRINGLE, M.S., KOPPERS, A.A.P. & SCHEEVERS, R. 1995. Argon geochronology of small samples using the Vulkaan argon laser-probe. *Proceedings of the Royal Netherlands Academy of Arts and Sciences*, **98**, 185–219.

WILLIAMS, D.M., HARKIN, J., ARMSTRONG, H.A. & HIGGS, K.T. 1994. A late Caledonian mélange in Ireland: implications for tectonic models. *Journal of the Geological Society, London*, **151**, 307–314.

WINCHESTER, J.A. 1992. Comment .on 'Exotic metamorphic terranes in the Caledonides: Tectonic history of the Dalradian block, Scotland'. *Geology*, **20**, 764.